

Chemical kinetics in carbon depositing d.c.-arc jet CVD reactors

Yu.A. Mankelevich^{a,*}, N.V. Suetin^a, M.N.R. Ashfold^b, W.E. Boxford^b, A.J. Orr-Ewing^b, J.A. Smith^b, J.B. Wills^b

^aNuclear Physics Institute, Moscow State University, 119992 Moscow, Russia

^bSchool of Chemistry, University of Bristol, Cantock's Close, Bristol, BS8 1TS, UK

Abstract

Experimental and theoretical studies of the behaviour of hydrocarbon species in d.c.-arc jet chemical vapour deposition reactors are reported, as a function of carbon source gas flow rate. CH(X) and C₂(a) radical number densities have been measured in absorption (by cavity ring-down spectroscopy) and via their optical emission in an arc jet plume operating with a standard CH₄/H₂/Ar feedstock gas mixture. The C₂(a) radical number density is seen to exhibit a linear (or sub-linear) dependence on CH₄ flow rate, in accord with previous findings (J. Appl. Phys. 82 (1997) 2072) for both C₂(a) and C₃(X) radicals in a lower power d.c.-arc jet. The present findings, together with the comprehensive set of earlier experimental data on gas velocity and gas temperature measurements (Diam. Relat. Mater. 7 (1998) 165; Plasma Sources Sci. Technol. 10 (2001) 595) have been used in developing a model of the plasma plume. The present calculations suggest that the observed high diamond growth rates (>50–100 μm/h) are most probably related to atomic C, which is present at concentrations as high as 10¹⁴ cm⁻³, though C₂ species are calculated to be present at comparable abundance and thus may also contribute to growth. The high temperatures (~3200 K) and large H₂ dissociation fraction (tens of percent) result in fast conversion of the input CH₄ into C atoms as a result of H-shifting reactions of the form: CH_x + H ⇌ CH_{x-1} + H₂. The plasma-chemical reaction mechanism and thermochemical data developed here goes some way to unravelling the complex inter-conversion mechanisms linking C₁, C₂ and C₃ hydrocarbons and changing the extent of H-saturation via series of H-shifting reactions of the form: C_xH_y + H ⇌ C_xH_{y-1} + H₂, (x=1–3). The simplified model for carbon source gas incorporation into the free stream introduced in this work is shown to overestimate the C₂(a) density but to provide a very reasonable description of CH densities measured in the Bristol d.c.-arc jet, and to reproduce well the C and CH radical absorbances and broadband absorbance at 248 nm reported in an expanding cascaded arc jet reactor operating with Ar/C₂H₂ at Eindhoven University of Technology.

© 2002 Elsevier Science B.V. All rights reserved.

Keywords: DC-arc jet; H/C chemistry; Modelling; Cavity ring-down spectroscopy

1. Introduction

Polycrystalline diamond and diamond-like carbon can be deposited in d.c.-arc jet chemical vapour deposition (CVD) reactors at exceptional growth rates $G > 100$ μm/h [1–3]. The gas-phase plasma chemistry prevailing in mixtures of hydrocarbons, hydrogen and inert gases involves complex mechanisms including radical production and larger hydrocarbon (C₃H_y, C₄H_y) formation processes. Over the last decade many experimental data for the plume in different d.c.-arc jet reactors have been reported, including spatially resolved measurements of

gas temperature and flow velocities [4–6] and absolute and relative species concentrations for H, C, CH, CN, C₂, C₃ and electrons [6–12]. Variations in radical concentration have been studied as functions of operating parameters (e.g. input power, hydrocarbon flow rate), and both axial and radial position within the free plume, (using laser induced fluorescence [9] or inverse Abel transform reconstruction of optical emission measurements [2]). Radially averaged concentrations of CH and C₂ radicals have recently been obtained using another non-invasive laser method, cavity ring-down spectroscopy (CRDS) [11,12]. Chemical mechanisms have been proposed for the gas plume of a d.c.-arc jet [4,13–15] but, to our knowledge, these numerical models have not yet been able to explain various of the

*Corresponding author. Tel.: +7-95-9394102; fax: +7-95-9390909.

E-mail address: ymankelevich@mics.msu.su (Y. Mankelevich).

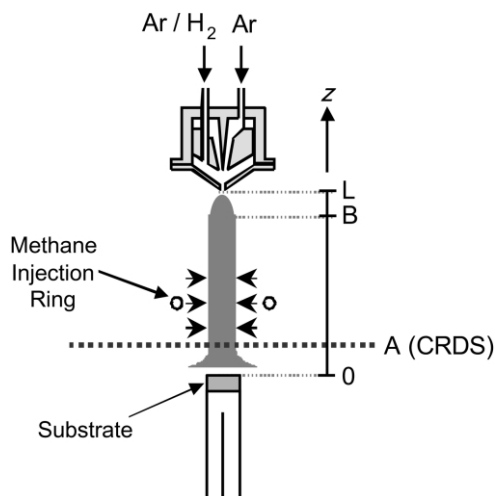


Fig. 1. Schematic cross-sectional view of the N-torch head, plasma plume and substrate holder in the Bristol d.c.-arc jet reactor.

experimental observations and measurements. In particular, the measured linear (or fractional power) dependence of C_2 [9,11] and C_3 [9] number densities with increasing CH_4 flow rate still needs to be explained, and the overall reaction mechanism requires extension to accommodate heavier species like C_3 , higher hydrocarbons, and ions, in an internally consistent manner.

The combined programme of experiment and modelling described in this article is designed as a first test of an extended plasma chemistry scheme and its related thermochemistry, and to provide a detailed interpretation of the available experimental data from various d.c.-arc jet CVD set-ups. Details of the 10 kW d.c.-arc jet reactor operated in Bristol with $CH_4/H_2/Ar$ mixtures and the CRDS radical detection schemes have been presented elsewhere [11]. The experimental part of this study involves use of CRDS to provide absolute number density measurements of $CH(X)$ and $C_2(a)$ radicals as a function of process conditions (e.g. CH_4 flow rate and input power). Results obtained in the free stream region of the gas plume sufficiently distant from the substrate to avoid perturbations from reflected gas (i.e. $z > 5$ mm) are compared with output from the developed model. Here we describe a quasi one-dimensional (1-D) model of the free plasma plume. This model provides species densities as a function of distance from the nozzle and incorporates certain fitting parameters to accommodate two-dimensional (2-D) effects such as radial diffusion and recirculation. The numerical simulations highlight the need for full 2-D (r, z) model development.

2. Model of d.c.-arc jet gas plume

Fig. 1 presents a schematic illustration of the d.c.-arc jet reactor, and defines the various regions of the plume treated in the model. A spiral jet secondary stream of

Ar/H_2 (typical flow rates of 1.4 slm Ar and 1.8 slm H_2) is incorporated into a primary Ar plasma flow (typical flow rate of 10 slm Ar) in the N-torch of a twin torch assembly. A further 0.75 slm Ar is introduced through the smaller companion P-torch (not shown) and the input power to the discharge is typically ~ 6 kW. Gas pressures behind the nozzles (both of 0.38 cm diameter) are 4 bar for the primary flow and 3 bar for the secondary flow. These gas flows are mixed and undergo initial expansion in the intermediate chamber of the N-torch, prior to expansion into the main reaction chamber through the output nozzle (throat diameter $d = 0.25$ cm). The pressure P in the reaction chamber is maintained at 50 Torr. Methane is introduced into the Ar/H_2 plasma through an annular injection ring positioned 10 cm downstream from the output nozzle. A coordinate system is chosen in which the symmetry axis of the plume (with origin at the substrate) is the z axis. CRDS measurements are performed along an axis orthogonal to z , at different distances A from the substrate.

The model aims to describe the plasma-chemical transformations within the gas as it evolves from the output nozzle, through the expansion region (LB in Fig. 1) and into the free plume region (BA), wherein the flow parameters (gas pressure and temperature, and axial velocities) remain essentially constant [4,10,11], at least for pressures in the reaction chamber of 20–50 Torr. The axial gas velocity in the LB region initially increases to some supersonic velocity due to expansion and then, after shock wave formation, relaxes to the free plume velocity v_p . We recognise that the axial velocity has a radial dependence [4], and v_p hereafter refers to the plume velocity averaged over its cross-sectional area. We also need to know how the pressure evolves from its (unmeasured) value P_L at the output nozzle to the free plume pressure $P = 50$ Torr. The gas pressure P_L at the nozzle exit may be estimated using the known total flow rate $Q = 13.2$ slm = 220 sccs and assuming that the gas temperature, T_L , in this region is close to the free plume temperature $T_p = 3200$ K [11]. Using flow conservation conditions, we obtain:

$$P_L [\text{torr}] = Q [\text{sccs}] \times 760 T_L / (v_L \times 273 \times S), \quad (1)$$

where v_L is the velocity at the exit of the output nozzle, and the nozzle cross-sectional area $S = \pi d^2/4$. v_L will equal the local sound velocity c_s ($c_s = 10^5$ cm/s for our conditions) if the pressure ratio of the high- and low-pressure regions exceeds a value of 2.1 [6]. Thus we obtain $P_L = 490$ Torr and $P_L/P \sim 9.5$ (i.e. > 2.1).

To compare the calculated results with the CRDS measurements at $z = A$ we need an estimate of the residence time $t = (B - A)/v_p$. v_p is estimated as follows. We assume an effective plume diameter $D = 1.2$ cm based on the earlier optical emission measurements

which showed that a cylinder with diameter 1 cm incorporated >90% of the emitting $C_2(d)$ radicals [2,11]. Using the same flow conservation condition as above for the free plume with gas temperature $T_p = 3200$ K and pressure $P = 50$ Torr, we obtain $v_p = 3.4 \times 10^4$ cm/s and, consequently, a residence time $t = 0.38$ ms for a typical B–A separation of 13 cm. Note that the length of the expansion region is much smaller ($L - B \sim 0.5 D$).

Another problem when constructing such a simplified model is how to introduce the carbon source gas into the reactive mixture. It is evident that during operation the whole reaction chamber, except for the near-hot-plume region, is filled by a mixture comprising mainly stable species such as CH_4 , Ar and H_2 in proportions close to their respective flow rates. Radial diffusion ensures that methane and molecular hydrogen are introduced into the hot plume along its entire length, save for the region of initial fast expansion near $z = L$. Methane injection is thus modelled via a CH_4 source term in the set of species conservation equations. The rate of this source is chosen so as to ensure that the ratio of carbon balance to argon density at $z = A$ matches the input CH_4/Ar flow rate ratio. This simplified approach is an attempt to describe the much more complex real situation which must include a coaxial transition layer between the hot plume and the cold regions and allow for diffusional transfer of radicals into and from the hot plume. A 2-D (z, r) model designed to reproduce correctly the large temperature and species gradients in this transition layer is under development.

The set of non-stationary conservation equations for species densities is integrated numerically to provide radially averaged species densities in the gas plume as a function of time or, equivalently, axial coordinate (z) if the gas velocity dynamics are known. Several chemical reaction mechanisms have been proposed to describe the gas plumes of d.c.-arc jet reactors [4,13–15], but the necessary complex plasma chemistry and thermochemistry are still far from complete and need extension and validation. We have developed our own chemical mechanism combining four main blocks for species:

- i. H, H_2 , CH_y ($y = 0-4$) and C_2H_y ($y = 1-6$), taken from the GRI-Mech 3.0 mechanism [16],
- ii. C_3H_y ($y = 3,4$), C_4H_y ($y = 1-4$) and C_6H_y from CH_4 [17] and C_2H_2 [18] pyrolysis mechanisms,
- iii. $C_2(X)$, $C_2(a)$ and C_3H_y ($y = 0-2$) [19–22],
- iv. ion conversion and electron–ion recombination reactions [3,12,23,24].

C_2 radicals in their ground and low-lying metastable excited ($a^3\Pi_u$) states are separated in block (iii) in recognition of their very different reactivities with H_2 and other species [19]. In addition, the separation allows more detailed comparison with the CRDS measurements of $C_2(a)$. Thermochemical data for reactions in blocks

(ii) and (iii) at several temperatures were taken from Refs. [18,20] and interpolated, but these assumed temperature dependences still need validation. As a result, the current reaction mechanism (blocks (ii), (iii) and key parts of block (iv)) and related rate coefficients are listed in Table 1.

The precise species distribution within the d.c.-arc discharge and the intermediate chamber used to establish the initial conditions at $z = L$ appears not to be particularly important. We have assumed that the degree of hydrogen dissociation in the intermediate chamber is close to its equilibrium value at $T = 3200$ K and $P_L = 490$ Torr ($[H]/[H_2] = 1.25$ for our typical Ar/ H_2 flow rate ratio of 6.33). Calculations show that the equilibrium charged particle distribution of species concentrations is established rapidly in the intermediate chamber and within the expansion region LB and that varying the initial (unknown) degree of ionisation degree at $z = L$ (over the wide range 0.001–20%) has negligible effect on the charged and neutral species concentrations at the beginning of the free plume region ($z = B$). For example, we find the density distribution of various of the key species at $z = B$ —e.g. $[Ar] = 1.24 \times 10^{17}$, $[H] = 1.51 \times 10^{16}$, $[H_2] = 1.21 \times 10^{16}$, $[e] = [ArH^+] = 2.41 \times 10^{11}$ cm $^{-3}$ for the Ar/ H_2 flow rate ratio of 6.33 used here—irrespective of the assumed degree of ionisation at $z = L$. Thus, we conclude that quite significant changes in the d.c.-arc discharge input power will have but modest effects on the gas temperature and the degree of hydrogen dissociation in the intermediate region and thus on the various species concentrations in the reaction chamber.

3. Calculated results and CRDS measurements

Here we compare $C_2(a)$ and CH(X) number densities measured by CRDS in arc jet activated $CH_4/H_2/Ar$ mixtures at $z = A$ [11], as a function of methane flow rate, with the results of calculations. The calculated variations of the different C_xH_y species densities shown in Figs. 2 and 3 accord well with the available experimental observations. Indeed, agreement in the case of CH is essentially quantitative, but we note that the model predicts $C_2(a)$ concentrations that are some 7.5 times larger than observed experimentally. This overestimation of $C_2(a)$ concentrations might be a consequence of the neglect of radial diffusional loss in the 1-D model, or improper thermochemical data and modelling of equilibration between $C_2(X)$ and $C_2(a)$ radicals, or of the conversion of such radicals to higher C_xH_y ($x > 2$) species under the prevailing experimental conditions. Spatially resolved CRDS measurements of the absolute concentrations of both $C_2(X)$ and $C_2(a)$ radicals in the d.c.-arc jet reactor are planned, which will provide a more stringent test of future 2-D models of the plasma plume. CH_4 molecules incorporated into the hot plume

Table 1
Reaction mechanism included in blocks (ii)–(iv)

Reactions	A	<i>n</i>	<i>E_A</i>
C+CH	⇌ C ₂ (a)+H	2E+14	0
C+CH ₄	⇌ C ₂ H ₃ +H	5E+13	0
C+C ₂ H	⇌ C ₃ +H	1.6E+14	0
C+C ₂ H ₂	⇌ C ₃ H+H	1.6E+14	0
CH+C ₂ (a)	⇌ C ₃ +H	1E+14	0
CH+C ₂ (X)	⇌ C ₃ +H	2E+14	0
CH+C ₂ H	⇌ C ₃ H+H	2E+14	0
CH+C ₂ H ₂	⇌ C ₃ H ₂ +H	2E+14	0
CH ₂ (S)+C ₂ H ₂	⇌ C ₃ H ₃ +H	2E+14	0
C ₂ (X)+H ₂	⇌ C ₂ H+H	8.4E+11	0
C ₂ (a)+C ₂ (a)	⇌ C ₃ +C	3.2E+14	0
C ₂ (a)+C ₂ (X)	⇌ C ₃ +C	3.2E+14	0
C ₂ (X)+C ₂ (X)	⇌ C ₃ +C	3.2E+14	0
C ₂ (a)+CH ₂	⇌ C ₃ H+H	1.2E+14	0
C ₂ (a)+CH ₃	⇌ C ₃ H ₂ +H	1.2E+14	0
C ₂ (a)+CH ₄	⇌ C ₃ H ₃ +H	1.2E+14	0
C ₂ (a)+C ₂ H	⇌ C ₄ +H	6E+13	0
C ₂ (a)+C ₂ H ₂	⇌ C ₄ H+H	6E+13	0
C ₂ (X)+CH ₂	⇌ C ₃ H+H	2E+14	0
C ₂ (X)+CH ₃	⇌ C ₃ H ₂ +H	2E+14	0
C ₂ (X)+CH ₄	⇌ C ₃ H ₃ +H	2E+14	0
C ₂ (X)+C ₂ H	⇌ C ₄ +H	2E+14	0
C ₂ (X)+C ₂ H ₂	⇌ C ₄ H+H	2E+14	0
C ₂ (a)+M	⇌ C ₂ (X)+M	1.8E+10	0
C ₂ H+C ₂ H	⇌ C ₄ H+H	1E+14	0
C ₂ H+C ₂ H ₂	⇌ C ₄ H ₂	8.32E+21	-3
C ₂ H+C ₂ H	⇌ C ₂ H ₂ +2(a)	1E+13	0
C ₂ H+CH ₄	⇌ C ₃ H ₄ +H	1.2E+14	0
C ₂ H+CH ₃	⇌ C ₃ H ₃ +H	1.2E+14	0
C ₃ +CH	⇌ C ₄ +H	2E+14	0
C ₃ +CH ₂	⇌ C ₄ H+H	2E+14	0
C ₃ +CH ₃	⇌ C ₄ H ₂ +H	2E+14	0
C ₃ +CH ₄	⇌ C ₄ H ₃ +H	3E+8	0
C ₃ H+H	⇌ C ₃ +H ₂	1E+14	0
C ₃ H ₂ +H	⇌ C ₃ H+H ₂	1E+14	0
C ₂ H+M	⇌ C ₂ (a)+H+M	1.74E+35	-5.16 114 000
C ₂ +M	⇌ C+C+M	1.5E+16	0 142 400
CH ₂ +CH ₂	⇌ C ₂ H ₂ +H+H	1.2E+14	0 800
C ₂ H ₂ +C ₂ H ₂	⇌ C ₄ H ₄	3.9E+12	0 32 600
C ₂ H ₂ +C ₂ H ₂	⇌ C ₄ H ₂ +H ₂	1E+14	0 52 200
C ₂ H ₂ +C ₂ H ₂	⇌ C ₄ H ₃ +H	1.4E+15	0 65 500
C ₄ H ₄	⇌ C ₄ H ₂ +H ₂	1.1E+13	0 75 000
C ₄ H ₃ +H	⇌ C ₄ H ₂ +H ₂	8.1E+13	0 0
C ₂ H+C ₂ H ₂	⇌ C ₄ H ₂ +H	1.2E+14	0 0
C ₂ H+C ₄ H ₂	⇌ C ₆ H ₂ +H	1.2E+14	0 0
C ₄ H ₂	⇌ C ₄ H+H	8.9E+17	0 131 600
C ₆ H ₂	⇌ C ₆ H+H	8.9E+13	0 112 100
C ₄ H+C ₂ H ₂	⇌ C ₆ H ₂ +H	1.2E+14	0 0
C ₄ H+H ₂	⇌ C ₄ H ₂ +H	4.1E+5	2.4 200
C ₆ H+H ₂	⇌ C ₆ H ₂ +H	4.1E+5	2.4 200
C ₄ H ₂ +C ₂ H ₂	⇌ C ₆ H ₂ +H ₂	1E+14	0 52 200
CH ₂ (S)+C ₂ H ₂	⇌ C ₃ H ₃ +H	8E+13	0 0
C ₃ H ₃ +CH ₂	⇌ C ₄ H ₄ +H	4E+13	0 0
Ar ⁺ +H ₂	→ ArH ⁺ +H	6E+14	0 0
Ar ⁺ +C ₂ H ₂	→ C ₂ H ₂ ⁺ +Ar	1E+14	0 0
Ar ⁺ +C ₂ H	→ C ₂ H ⁺ +Ar	1E+14	0 0
Ar ⁺ +CH	→ CH ⁺ +Ar	1E+14	0 0
Ar ⁺ +C ₂ (a)	→ C ₂ ⁺ +Ar	1E+13	0 0
Ar ⁺ +C ₂ (a)	→ C ⁺ +C+Ar	1E+14	0 0
Ar ⁺ +C ₂ (X)	→ C ₂ ⁺ +Ar	1E+13	0 0
Ar ⁺ +C ₂ (X)	→ C ⁺ +C+Ar	1E+14	0 0
Ar ⁺ +C	→ C ⁺ +Ar	1E+9	0 0
ArH ⁺ +e	→ Ar+H	3.6E+16	0 0

Table 1 (Continued)

Reactions	A	<i>n</i>	<i>E_A</i>
C ₂ H ₂ ⁺ +e	→ C ₂ H+H	1.58E+19	-0.68 0
C ₂ H ⁺ +e	→ CH+C	1.41E+18	-0.5 0
CH ⁺ +e	→ C+H	9.39E+17	-0.42 0
C ₂ ⁺ +e	→ C+C	3.13E+18	-0.5 0
H ⁺ +e+e	→ H+e	1.15E+39	-4.3 0
Ar ⁺ +e+e	→ Ar+e	1.15E+39	-4.3 0
C ⁺ +e+e	→ C+e	1.15E+39	-4.3 0
H ⁺ +e+M	→ H+M	5.6E+27	-2.5 0
Ar ⁺ +e+M	→ Ar+M	5.6E+27	-2.5 0
C ⁺ +e+M	→ C+M	5.6E+27	-2.5 0

Rate coefficient $k = AT^n \exp(-E_A/RT)$, units: cal, mol, K, cm, s. M is a third body.

are the primary source of hydrocarbons, which then participate in a complex variety of reaction pathways. The dependence of the various C₁, C₂ and C₃ hydrocarbon species concentrations with CH₄ flow rate is the result of a complex balance between these numerous reactions. The most important of these are the families of H-shifting reactions C_xH_y+H ⇌ C_xH_{y-1}+H₂ (*x*=1–3) and reactions that link between the various C₁, C₂ and C₃ hydrocarbon groups such as:



The high C and H atom concentrations, and the high H/H₂ ratio, predicted by the modelling studies (Fig. 3) are all likely contributory factors to the high growth rates observed when using d.c.-arc jet reactors for diamond film growth. Building on the approach used in [25], the growth rate *G* of (100) diamond from CH₃ radicals at typical substrate temperatures *T_s*=1200 K can be expressed by the formula:

$$G(\mu\text{m/h}) = 3.84 \times 10^{-14} T_{\text{ns}}^{0.5} [\text{CH}_3] / (40 + 0.0324 [\text{H}_2] / [\text{H}]) \quad (9)$$

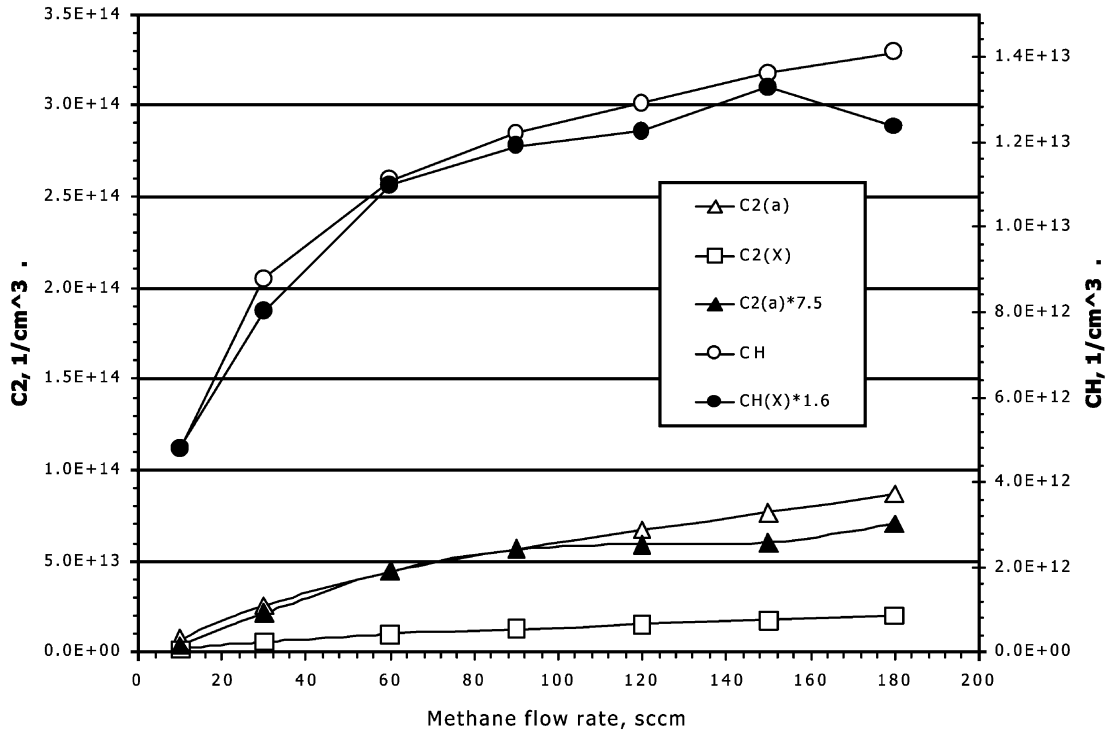


Fig. 2. Calculated $C_2(a)$, $C_2(X)$ and CH densities (open symbols) and $C_2(a)$ and $CH(X)$ column densities measured in the Bristol d.c.-arc jet reactor (filled symbols), as a function of input CH_4 flow rate. Note that the measured $CH(X)$ and $C_2(a)$ densities have been multiplied by a factor of 1.6 and 7.5, respectively, to aid comparison with the calculated trend.

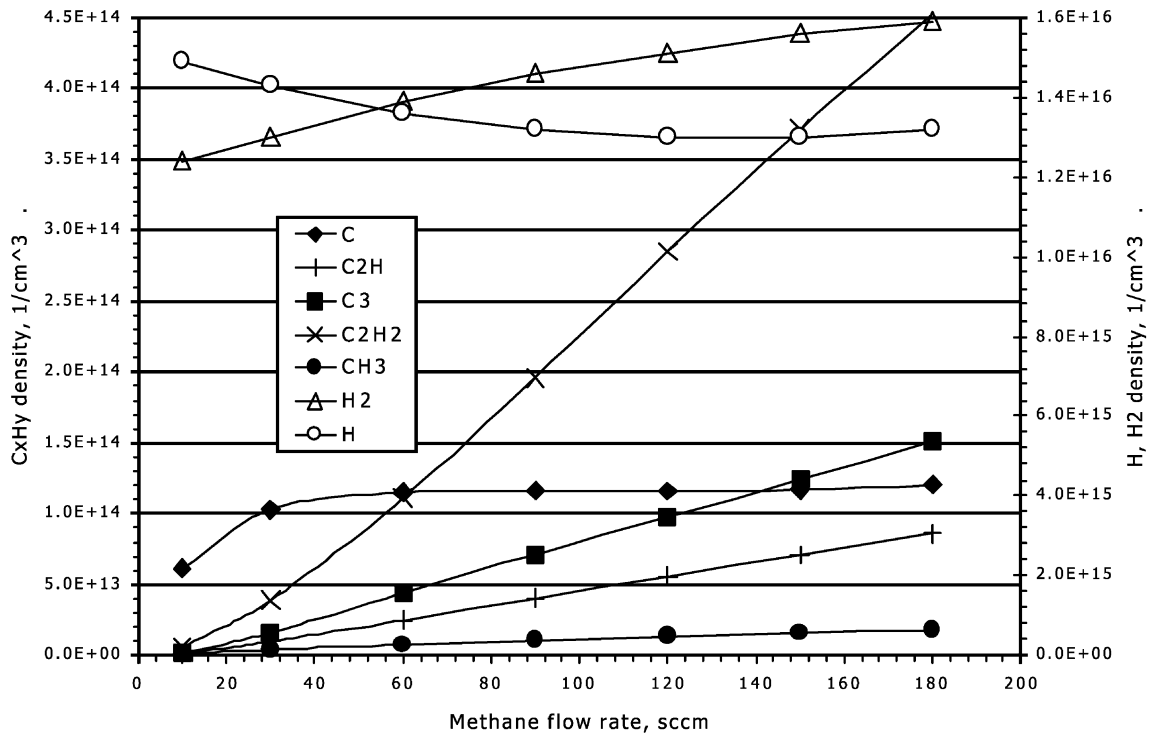


Fig. 3. Variation of the calculated C_xH_y species densities with added CH_4 .

Recognising that incorporation of C atoms into the growing film is more likely to be proportional to the formation rate of the free surface radical sites rather than site pairs as for CH₃ incorporation [25] we estimate the corresponding growth rate from C atoms for $T_s = 1200$ K as

$$G(\mu\text{m/h}) = 3.84 \times 10^{-14} T_{\text{ns}}^{0.5} [\text{C}] / (6.33 + 0.00256 [\text{H}_2] / [\text{H}]) \quad (10)$$

and obtain $G = 35$ $\mu\text{m/h}$ for our typical experimental conditions, i.e. a methane flow rate of 60 sccm and a gas temperature just above the substrate $T_{\text{ns}} \sim 4000$ K [11]. Under these conditions, the carbon atom number density [C] is determined mainly by the equilibrium



and is thus proportional to the local CH number density and the $[\text{H}]/[\text{H}_2]$ ratio. The [H] and $[\text{H}_2]$ densities in the free plume depend on the extent of thermal dissociation of H₂ and the reverse association process



in the intermediate chamber at high pressures. In the free plume, H atom consumption through reaction with hydrocarbons increases with increasing CH₄ flow rate and [H] thus falls slowly, as seen in Fig. 3. The calculations show that the C atom number density initially rises but thereafter remains essentially constant with increasing CH₄ flow rate—a consequence of the fact that the increase in [CH] is largely offset by the falling $[\text{H}]/[\text{H}_2]$ ratio. Since C atoms participate in all of the most important formation reactions for C₂ and C₃ hydrocarbons, this finding that [C] is only weakly dependent on the CH₄ flow rate provides a ready explanation for the (at first sight surprising) observation that both C₂(a) and C₃ radical concentrations scale, at most, linearly with increasing input [CH₄]. The model developed thus far predicts concentrations of C₂(a) that exceed those of C₂(X), in accordance with previous predictions [9,11] that the combined effect of the greater reaction rate of C₂(X) with H₂, and Boltzmann partitioning between the two states at elevated temperatures, will favour a higher steady state concentration of C₂(a). In concluding this section, we note that plasma reactions are not important radical sources in the d.c.-arc jet reactor under study; concentrations of electrons and ArH⁺ ions at $z = A$ are calculated to have declined to $\sim 3.8 \times 10^{10} \text{ cm}^{-3}$ as a result of electron–ion recombination processes in the plume.

To test our model under alternative conditions, where plasma sources are of primary importance, we have also performed initial simulations of an argon expanding

cascaded arc plasma with downstream addition of acetylene operated in the group of Schram and van de Sanden [3,12]. A description of this d.c.-arc jet reactor, which is used for deposition of hydrogenated amorphous carbon films, and details of CRDS measurements in this reactor, have been presented elsewhere [12,26]. Briefly, an arc argon plasma (0.2–0.5 bar) expands into a low-pressure reaction chamber (0.3 mbar). The arc current is 48 A and the corresponding Ar⁺ ion and Ar neutral flow rates are ~ 6 and 100 sccs, respectively, [12]. C₂H₂ is incorporated into the plasma plume downstream. Charge exchange reactions between Ar⁺ ions and C_xH_y molecules, followed by the dissociative recombination of ions with electrons, constitute the primary radical source [3,12].

Fig. 4 displays the results of our model calculations along with experimentally measured C atom and CH radical absorbances, and a broadband absorption (BBA) monitored at 248 nm, each measured by CRDS as a function of C₂H₂ flow rate, along an axis that intersects the plasma axis at a point half way between the arc and the substrate holder (i.e. 30 cm from the nozzle) [26]. The measured trends in [C] and [CH] can be reproduced well by the model assuming a residence time of 1.3 ms and constant gas temperature of 1800 K, though we caution that the experimental measurables in both cases are absorbances and, without due allowance for different oscillator strengths of the various electronic transitions, do not represent either relative or absolute number densities. The experimental data have thus been scaled (vertically) so as to match the calculated number densities. The BBA, that extends from at least 248 nm up to 517 nm, has been attributed to various unknown hydrocarbons [12,26]. The model calculations summarised in Fig. 4 suggest that C₃H radicals may well be important contributors to the BBA.

4. Conclusions

A quasi 1-D model of the expansion region and free plume of a d.c.-arc jet CVD reactor has been developed. The model offers explanations for experimental observations of the way in which the number densities of various hydrocarbon species (e.g. CH, C₂) present in the plume vary with the input flow rate of the carbon source (CH₄ or C₂H₂). The plasma–chemical reaction sequences and thermochemical data developed in this study have allowed us to unravel details of the complex mechanisms whereby C₁, C₂ and C₃ hydrocarbon species interconvert both within (by H-shifting reactions), and between, the respective C_x families. The high diamond growth rates, G , achievable with d.c.-arc jet reactors are most likely attributable to the high C and H atom densities present in the plume, though we recognise that the predicted C₂ concentrations are such that we cannot exclude contributions from these species to film growth.

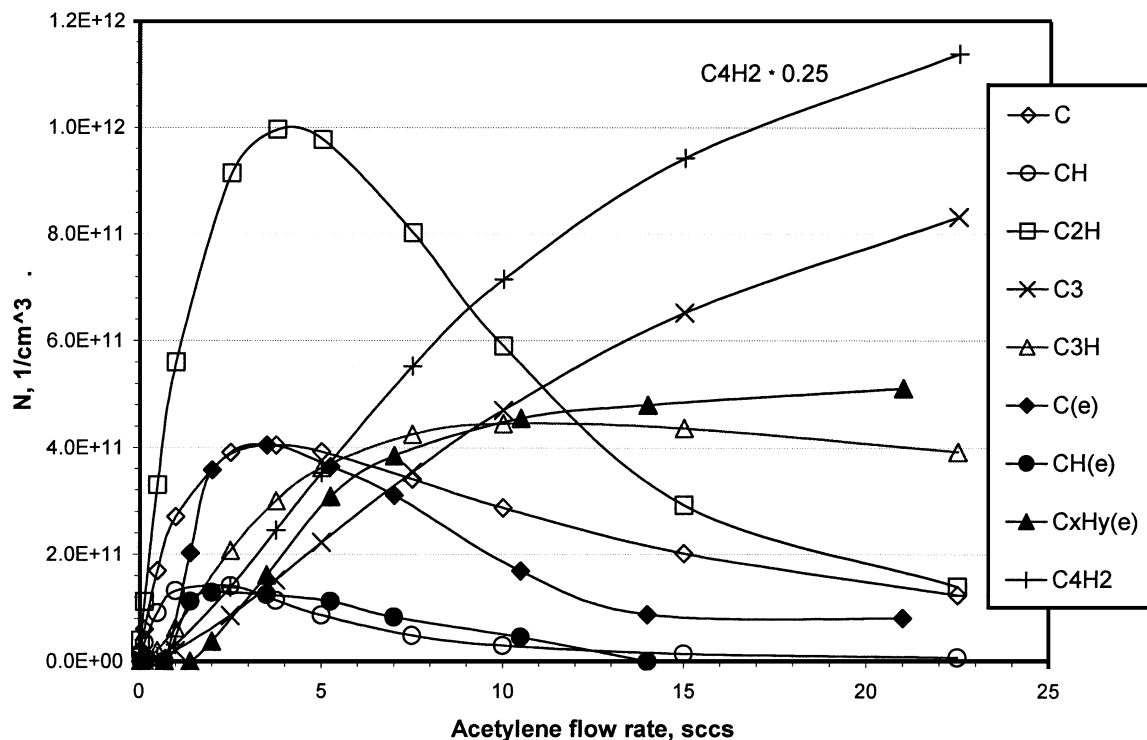


Fig. 4. Variation of the calculated densities of selected atoms and molecular species (open symbols) in the cascaded arc Ar/C₂H₂ plasma at EUT. Note that the C₄H₂ densities have been multiplied by a factor of 0.25. Also shown (solid symbols, and indicated with an (e) in the accompanying legend) are measured absorbances for C, CH and the BBA (monitored at 248 nm and attributed to C_xH_y species). These have been independently scaled, vertically, to match the model calculations.

The present model calculations suggest values of [H] $\sim 1.4 \times 10^{16}$ and [C] $\sim 10^{14}$ cm⁻³ in the free plume of the Bristol d.c.-arc jet reactor (in which $G \sim 100$ $\mu\text{m}/\text{h}$); we anticipate that [C] near the substrate will be several times higher still, as observed for the case of CH and C₂(a) radicals in this reactor [11]. Measured C₂(a) and CH number densities (in the Bristol d.c.-arc jet) and absorption by C atoms and CH radicals, and a BBA (monitored at 248 nm) attributed to unidentified higher hydrocarbons (in an argon expanding cascaded arc jet reactor at Eindhoven University of Technology), are reasonably described by the calculations which introduce a simplified approach for treating carbon source gas incorporation into the free stream.

Acknowledgments

We are grateful to the EPSRC for equipment grants and for the award of a Senior Research fellowship (MNRA), a post-doctoral research assistantship (JAS) and a studentship (JBW). We are also most grateful to De Beers Industrial Diamonds for the long term loan of the d.c.-arc jet reactor, to the Royal Society for a Joint Project Grant that enables the Bristol–Moscow collaboration, to J. Benedikt for discussions about the EUT experimental data (YAM), and to NATO for the award of SfP grant N974354 (YAM).

References

- [1] N. Ohtake, M. Yoshikawa, *J. Electrochem. Soc.* 137 (1990) 717.
- [2] J.A. Smith, K.N. Rosser, H. Yagi, M.I. Wallace, P.W. May, M.N.R. Ashfold, *Diam. Relat. Mater.* 10 (2001) 370.
- [3] J.W.A.M. Gielen, M.C.M. van de Sanden, P.R.M. Kleuskens, D.C. Schram, *Plasma Sources Sci. Technol.* 5 (1996) 492.
- [4] W. Juchmann, J. Luque, J. Wolfrum, J.B. Jeffries, *Diam. Relat. Mater.* 7 (1998) 165.
- [5] E.A. Brinkman, G.A. Raiche, M.S. Brown, J.B. Jeffries, *Appl. Phys. B* 64 (1997) 689.
- [6] R. Engeln, S. Mazouffre, P. Vankan, D.C. Schram, N. Sadeghi, *Plasma Sources Sci. Technol.* 10 (2001) 595.
- [7] E.A. Brinkman, K.R. Stalder, J.B. Jeffries, *J. Appl. Phys.* 81 (1997) 1093.
- [8] W. Juchmann, J. Luque, J.B. Jeffries, *J. Appl. Phys.* 81 (1997) 8052.
- [9] J. Luque, W. Juchmann, J.B. Jeffries, *J. Appl. Phys.* 82 (1997) 2072.
- [10] J. Luque, W. Juchmann, E.A. Brinkman, J.B. Jeffries, *J. Vac. Sci. Technol. A* 16 (1998) 397.
- [11] J.B. Wills, J.A. Smith, W.E. Boxford, J.M.F. Elks, M.N.R. Ashfold, A.J. Orr-Ewing, *J. Appl. Phys.* 92 (2002) 4213.
- [12] J. Benedikt, K.G.Y. Letourneur, M. Wisse, D.C. Schram, M.C.M. van de Sanden, *Diam. Relat. Mater.* 11 (2002) 989.
- [13] M.E. Coltrin, D.S. Dandy, *J. Appl. Phys.* 74 (1993) 5803.
- [14] S.W. Reeve, W.A. Weimer, F.M. Cerio, *J. Appl. Phys.* 74 (1993) 7521.
- [15] B.W. Yu, S.L. Girshick, *J. Appl. Phys.* 75 (1994) 3914.

- [16] G.P. Smith, D.M. Golden, M. Frenklach, et al. Available from: http://www.me.berkeley.edu/gri_mech/.
- [17] D.I. Slovetskii, Yu.A. Mankelevich, S.D. Slovetskii, T.V. Rakhimova, Proceedings of Fifteenth International Symposium on Plasma Chemistry, vol. 2, France, 2001, pp. 715–719, *Chemistry of High Energy* 36 (2002) 64.
- [18] J.H. Kiefer, S.S. Sidhu, R.D. Kern, K. Xie, H. Chen, L.B. Harding, *Combust. Sci. Technol.* 82 (1992) 101.
- [19] H. Reisler, M.S. Mangir, C. Wittig, *J. Chem. Phys.* 73 (1980) 2280.
- [20] T. Kruse, P. Roth, *J. Phys. Chem.* 101 (1997) 2138.
- [21] R. Guadagnini, G.C. Schatz, S.P. Walch, *J. Phys. Chem.* 102 (1998) 5857.
- [22] D. Chastaing, S.D. Le Picard, I.R. Sims, I.W.M. Smith, *Astronomy Astrophys.* 365 (2001) 241.
- [23] D.K. Otorbaev, A.J.M. Buuron, N.T. Guerassimov, M.C.M. van de Sanden, D.C. Schram, *J. Appl. Phys.* 76 (1994) 4499.
- [24] Yu.P. Raizer, *Physics of a Gas Discharge*, Nauka, Moscow, 1987.
- [25] Yu.A. Mankelevich, A.T. Rakhimov, N.V. Suetin, *Diam. Relat. Mater.* 5 (1996) 888.
- [26] A. Rakhimov, A. Bogaerts (Eds.), NATO Sfp-974354 report, 2002, pp. 42.